Attractive Centers IV

Analytic Triangle Hearts, Centroidal Rays, and Nonlocal Constraints

Ismail Hammoudeh

September 2026; revised submission version

Abstract

Papers I and II develop, respectively, outer certificate regions and the global-extension problem on the isosceles stratum. This paper studies the analytic Heart at an arbitrary triangle: the convex locus of values attained by globally defined analytic invariant attractive center maps.

We derive an exact spectral criterion for affine rays through the centroid. For the boundary-wire center $X(10)$ it gives the sharp globally attractive segment from the incenter $X(1)$ through $X(2) = G$ to $X(10)$. Near the equilateral triangle, representation theory produces universal second- and third-order barycentric jets and necessary coefficient constraints. Normalized squared-side variables yield a complete two-generator module of polynomial equivariant weight perturbations and a first-jet semidefinite formulation. We prove that purely local jets add no value confinement away from the equilateral shape; stronger bounds require constraints coupling distinct shapes.

Using the globally attractive power family classified in Paper III, we prove that the analytic Heart has nonempty interior for an open dense set of scalene triangle shapes. A concrete 13–20–21 example illustrates the remaining inner–outer gap. Corrected ETC computations are reported only as counterexample-oriented reconnaissance: 594 formulas remain unrefuted after the Jacobian and isosceles filters, but none is asserted attractive without a global proof.

Contents

1 Introduction 3

2 Smooth triangle centers on shape space 3
- 2.1 Barycentric representation . . . 3
- 2.2 Two useful shape coordinates . . . 4
- 2.3 The Jacobian formula . . . 4

3 The smooth heart and its support function 5

4 Centroidal rays and an exact spectral theorem 5
- 4.1 The exact $X(1)$–$X(2)$–$X(10)$ affine family . . . 6

5 Universal near-equilateral structure 8
- 5.1 The equilateral slope bound . . . 8
- 5.2 Benchmarks . . . 10
- 5.3 Third-order refinement from the isosceles chest . . . 10

6 A complete polynomial covariant basis for analytic constructions 11

7 The first-jet semidefinite outer relaxation 13

8 Exploratory ETC evidence and reproducibility status 14

9 A genuinely two-dimensional analytic heart 15
- 9.1 The tangent of the power-center curve at the centroid . . . 15
- 9.2 The 13–20–21 diagnostic triangle . . . 16

10 Inner–outer support matching 17

11 Open problems 18

12 Conclusion 18

A Derivation of the equilateral second-order constraints 19

1 Introduction

Paper I established outer certificate regions for attractive centers, and Paper II isolated the global-extension problem on the isosceles symmetry stratum. The present paper studies the full two-dimensional attainable locus at a fixed scalene triangle. Its central tools are exact spectral tests along affine rays through the centroid, universal equivariant jets near the equilateral shape, polynomial covariants, and semidefinite first-jet relaxations [1, 2].

Standing domain convention: center rules extend continuously to all degenerate configurations and are analytic on the nondegenerate triangle domain. Finite response across excluded strata uses this extension. For a fixed triangle P, the analytic Heart is the set of values $X(P)$ of globally defined analytic invariant attractive center maps. Convex mixing of center maps makes this locus convex, but pointwise positive semidefinite jets alone do not guarantee that a local value extends to such a global map. We therefore develop certified inner families and compatible outer relaxations in parallel.

The main exact inner family lies on the classical line through the incenter, centroid, and boundary-wire center. A spectral radial theorem proves the sharp attractive segment from $X(1)$ through $X(2)$ to $X(10)$. Near the equilateral triangle, symmetry reduces arbitrary analytic center jets to a small number of universal coefficients. Normalized squared-side variables then produce a complete two-generator module of polynomial equivariant weight perturbations and a first-jet semidefinite formulation, whose local value constraints are redundant off the equilateral shape. Finally, the globally attractive power family classified in Paper III leaves the classical segment transversely at a generic triangle; convex mixing consequently proves that the analytic Heart has nonempty interior on an open dense set of scalene shapes.

All computational ETC statements are explicitly exploratory. A negative Jacobian eigenvalue or a violation of a proved chest inequality is a valid disproof, whereas survival of a finite scan is not evidence of global attractivity.

2 Smooth triangle centers on shape space

2.1 Barycentric representation

Let $A, B, C \in \mathbb{R}^2$ be noncollinear and put

$$a = |B - C|, \qquad b = |C - A|, \qquad c = |A - B|.$$

Every point of the affine plane has unique barycentric coordinates with respect to ABC. We follow the standard triangle-center barycentric conventions of Kimberling [4].

Proposition 2.1 (Invariant barycentric form)**.** *Let X be a continuous Euclidean- and similarity-equivariant center of nondegenerate triangles. Then*

$$X(A, B, C) = w_A(a, b, c)A + w_B(a, b, c)B + w_C(a, b, c)C, \qquad w_A + w_B + w_C = 1, \qquad (1)$$

where the weights are dimensionless. Permutation invariance is equivalent to permutation covariance of the weight vector. If X is C^r or analytic, so are the weights on the side-length shape domain.

Proof. The barycentric coordinates exist and are unique because A, B, C are affine independent. Translation and rotation leave them unchanged. Positive scaling changes all three side lengths by the same factor while leaving the weights unchanged, so they are homogeneous of degree zero. Uniqueness of barycentric coordinates transfers every vertex permutation to the same permutation of the weights. Regularity follows from solving the nonsingular affine coordinate system locally. □

For a globally attractive center, Paper I's convex-hull theorem implies

$$w_A, w_B, w_C \geq 0. \tag{2}$$

Thus nonnegative barycentric weights are a consequence of attractivity rather than an independent axiom.

2.2 Two useful shape coordinates

Two coordinate systems will be used for different purposes.

For local analysis near the equilateral triangle, define logarithmic shape coordinates

$$\ell_a = \log a, \quad \ell_b = \log b, \quad \ell_c = \log c, \qquad u_i = \ell_i - \frac{\ell_a + \ell_b + \ell_c}{3}. \tag{3}$$

Then

$$u_a + u_b + u_c = 0,$$

and similarity scaling disappears exactly.

For global polynomial constructions, put

$$Q = a^2 + b^2 + c^2, \qquad s_1 = \frac{a^2}{Q}, \quad s_2 = \frac{b^2}{Q}, \quad s_3 = \frac{c^2}{Q}. \tag{4}$$

Let

$$e_2 = s_1 s_2 + s_2 s_3 + s_3 s_1, \qquad e_3 = s_1 s_2 s_3.$$

Heron's identity gives

$$\frac{16\Delta^2}{Q^2} = 4e_2 - 1, \tag{5}$$

where Δ is the triangle area. Consequently the labelled nondegenerate shape domain is exactly

$$\mathscr{S} = \left\{ s_i > 0 : \; s_1 + s_2 + s_3 = 1, \quad e_2 > \frac{1}{4} \right\}. \tag{6}$$

The equilateral triangle is $s_1 = s_2 = s_3 = 1/3$, while $e_2 = 1/4$ is the ordinary degenerate boundary. The closure of (6) inside the unit simplex is compact.

2.3 The Jacobian formula

Write $w = (w_A, w_B, w_C)$ as a function of (a, b, c). Differentiating (1) with respect to A gives

$$J_A = w_A I_2 + (B - A)(\nabla_A w_B)^T + (C - A)(\nabla_A w_C)^T, \tag{7}$$

where differentiated normalization was used to eliminate the A-term. Since a is independent of A,

$$\nabla_A w_j = \frac{\partial w_j}{\partial b} \frac{A - C}{b} + \frac{\partial w_j}{\partial c} \frac{A - B}{c}. \tag{8}$$

The two cyclic formulas are analogous.

Proposition 2.2 (Smooth attractivity criterion)**.** *A C^1 invariant triangle center is attractive on the nondegenerate domain if and only if*

$$S_A = \operatorname{Sym} J_A \succeq 0, \qquad S_B = \operatorname{Sym} J_B \succeq 0, \qquad S_C = \operatorname{Sym} J_C \succeq 0 \tag{9}$$

throughout that domain, with continuous extension used when a finite vertex motion passes through an excluded degeneracy.

This is the Jacobian criterion of Paper I. Permutation covariance means that it is enough in principle to prove one vertex inequality for every *labelled* triangle: the other two follow by relabelling. For numerical work it is often preferable to calculate all three as an internal check.

A convenient canonical chart fixes

$$A = (0, 0), \qquad B = (1, 0), \qquad C = (x, y), \qquad y > 0. \tag{10}$$

Every oriented nondegenerate triangle is directly similar to one and only one point of this chart after choosing the ordered side AB.

3 The smooth heart and its support function

Definition 3.1 (Regularity-dependent heart)**.** For $r \in \{1, \infty, \omega\}$, the C^r attainable locus at P is

$$\mathcal{V}^r(P) = \{X(P) : X \in \mathcal{A}^r\}.$$

Because $\mathcal{A}^r$ is closed under convex mixing, $\mathcal{V}^r(P)$ is convex. We call any explicitly certified convex subset a C^r *heart.* Its closure is denoted $\overline{\mathcal{V}^r(P)}$.

The closures satisfy

$$\overline{\mathcal{V}^\omega(P)} \subseteq \overline{\mathcal{V}^\infty(P)} \subseteq \overline{\mathcal{V}^1(P)}.$$

Whether these three closed loci agree is one of the basic open questions.

A closed convex locus is determined by its support function

$$h_P^r(n) = \sup_{X \in \mathcal{A}^r} n \cdot X(P), \qquad \|n\| = 1. \tag{11}$$

For a C^2 strictly convex boundary in the plane, with $n(\theta) = (\cos\theta, \sin\theta)$,

$$x(\theta) = h(\theta)n(\theta) + h'(\theta)(-\sin\theta, \cos\theta). \tag{12}$$

Thus inner and outer support estimates are a natural common currency: when a globally certified center attains an outer support bound, an exact exposed point of the closed heart has been proved.

Paper I supplies an outer region

$$\overline{\mathcal{V}^r(ABC)} \subseteq \mathcal{C}_{\text{std}}(ABC),$$

where $\mathcal{C}_{\text{std}}$ is the intersection of the triangle, the characteristic parallelogram, and the internal characteristic Napoleon triangle. The present paper will add stronger smooth outer relaxations and, more importantly, certified inner subsets.

4 Centroidal rays and an exact spectral theorem

Let

$$G = \frac{A + B + C}{3}$$

be the centroid. Given any C^1 invariant center Y, not necessarily attractive, consider the affine family

$$F_{\lambda,Y} = G + \lambda(Y - G). \tag{13}$$

Its vertex Jacobians satisfy

$$S_i(F_{\lambda,Y}) = \frac{1}{3}I_2 + \lambda\left(S_i(Y) - \frac{1}{3}I_2\right). \tag{14}$$

Define the global spectral extrema

$$m(Y) = \inf_{P,i} \lambda_{\min}(S_i(Y;P)), \qquad M(Y) = \sup_{P,i} \lambda_{\max}(S_i(Y;P)), \tag{15}$$

where P ranges over all nondegenerate labelled triangles.

Theorem 4.1 (Exact centroidal-ray criterion)**.** *The center map $F_{\lambda,Y}$ is globally attractive exactly for*

$$\lambda_-(Y) \le \lambda \le \lambda_+(Y),$$

where

$$\lambda_+(Y) = \begin{cases} \dfrac{1}{1-3m(Y)}, & m(Y) < 1/3, \\ +\infty, & m(Y) \ge 1/3, \end{cases} \tag{16}$$

and

$$\lambda_-(Y) = \begin{cases} -\dfrac{1}{3M(Y)-1}, & M(Y) > 1/3, \\ -\infty, & M(Y) \le 1/3. \end{cases} \tag{17}$$

The conventions are $\lambda_+ = 0$ if $m(Y) = -\infty$ and $\lambda_- = 0$ if $M(Y) = +\infty$.

Proof. Since (14) is a scalar affine function of the symmetric matrix $S_i(Y)$, the two matrices have the same eigenvectors. If μ is any eigenvalue of $S_i(Y)$, the corresponding eigenvalue of $S_i(F_{\lambda,Y})$ is

$$\frac{1}{3} + \lambda\left(\mu - \frac{1}{3}\right). \tag{18}$$

For $\lambda \ge 0$ this is minimized at the global lower spectral endpoint $m(Y)$; for $\lambda \le 0$ it is minimized at the global upper endpoint $M(Y)$. Solving the two scalar inequalities gives (16) and (17). If an endpoint is only approached and not attained, any strict violation outside the stated interval is still witnessed by a sufficiently close triangle. The Jacobian criterion completes the proof. $\square$

This theorem changes the computational radial problem from a repeated one-parameter PSD search into a global spectral-extremum problem for the original center Y.

4.1 The exact $X(1)$–$X(2)$–$X(10)$ affine family

The boundary-wire mass center of a triangle is

$$X(10) = \frac{(b+c)A + (c+a)B + (a+b)C}{2P}, \qquad P = a+b+c. \tag{19}$$

The incenter is

$$X(1) = \frac{aA + bB + cC}{P}. \tag{20}$$

They satisfy the exact affine identity

$$\boxed{X(1) = 3G - 2X(10).} \tag{21}$$

For motion of A, put

$$p = \frac{B-A}{c}, \qquad q = \frac{C-A}{b}, \qquad u = p \cdot q = \cos A.$$

Translate temporarily so that $A = 0$, hence $B = cp$ and $C = bq$. Since $\nabla_A c = -p$, $\nabla_A b = -q$, and $\nabla_A P = -(p+q)$, differentiation of the barycentric weights of (19) gives

$$\nabla_A w_B = \frac{-bp + (a+c)q}{2P^2}, \qquad \nabla_A w_C = \frac{(a+b)p - cq}{2P^2}.$$

Substitution in (7) yields

$$S_A(X(10)) = \frac{b+c}{2P} I - \frac{bc}{2P^2}(pp^T + qq^T) + \frac{c(a+c)+b(a+b)}{4P^2}(pq^T + qp^T). \tag{22}$$

Because p, q are unit vectors, $p+q$ and $p-q$ are orthogonal. Applying (22) to these directions gives the eigenvalues

$$\mu_+ = \frac{2P(b+c) + (1+u)[(b-c)^2 + a(b+c)]}{4P^2}, \tag{23}$$

$$\mu_- = \frac{(b+c)(1+u)}{4P}. \tag{24}$$

Both are strictly positive for a nondegenerate triangle.

Lemma 4.2 (Sharp spectrum of $X(10)$)**.** *Over all nondegenerate triangles and all moved vertices,*

$$0 < \lambda(S_i(X(10))) < \frac{1}{2},$$

and the closure of the global spectral range is $[0, 1/2]$.

Proof. The lower bounds follow from (23)–(24). For (24), $(b+c) < P$ and $(1+u) < 2$ give $\mu_- < 1/2$. For μ_+,

$$\frac{1}{2} - \mu_+ = \frac{2aP - (1+u)[(b-c)^2 + a(b+c)]}{4P^2}. \tag{25}$$

Put $s = P/2$ and

$$\xi = s - a, \qquad \eta = s - b, \qquad \zeta = s - c.$$

The numerator in (25) factors as

$$\frac{4\eta\zeta(\xi+\eta+\zeta)(2\xi+\eta+\zeta)}{(\xi+\eta)(\xi+\zeta)},$$

which is strictly positive for every nondegenerate triangle. Hence $\mu_+ < 1/2$.

As $A \to \pi$, $1+u \to 0$ and $\mu_- \to 0$. As $a \to 0$ with $b/c \to 1$, $u \to 1$ and $(b+c)/P \to 1$, so $\mu_- \to 1/2$. Thus the global infimum and supremum are exactly 0 and 1/2. □

Theorem 4.3 (Sharp classical heart segment)**.** *The affine center family*

$$F_\lambda = G + \lambda(X(10) - G)$$

is globally attractive if and only if

$$\boxed{-2 \le \lambda \le 1.} \tag{26}$$

At the three distinguished parameters,

$$F_{-2} = X(1), \qquad F_0 = G = X(2), \qquad F_1 = X(10).$$

Consequently, for every nondegenerate triangle,

$$[X(1), X(10)] \subseteq \mathcal{V}^\omega(ABC). \tag{27}$$

The interval (26) is maximal for this particular affine family of center maps.

Proof. Apply Theorem 4.1 with $m = 0$ and $M = 1/2$. The endpoint identities follow from (21). The functions involved are analytic on the nondegenerate triangle domain, so the entire segment is contained in the analytic attainable locus. □

The final sentence is important: the theorem does not assert that no other attractive center map can attain a point lying farther along the same geometric line at one fixed triangle. It asserts the exact maximal interval inside the globally defined affine family generated by G and $X(10)$.

5 Universal near-equilateral structure

The equilateral triangle is the unique shape at which every invariant center coincides. The way a heart opens when symmetry is broken is therefore a natural local invariant of the theory.

Let $u = (u_a, u_b, u_c)$ be the logarithmic shape variables (3). The plane

$$u_a + u_b + u_c = 0$$

is the standard two-dimensional representation of S_3.

Theorem 5.1 (Universal second-order equivariant expansion)**.** *Let $w(u) = (w_A, w_B, w_C)$ be the normalized barycentric weight vector of an analytic invariant triangle center. Near the equilateral point $u = 0$ there exist real constants κ and η such that*

$$\boxed{w_i = \frac{1}{3} + \kappa u_i + \eta \left(u_i^2 - \frac{1}{3} \sum_j u_j^2 \right) + O(\|u\|^3).} \tag{28}$$

No other independent first- or second-order equivariant terms occur.

Proof. At $u = 0$, permutation symmetry forces $w_i = 1/3$. The first variation is an S_3-equivariant linear endomorphism of the standard two-dimensional representation, hence is a scalar multiple of the identity on that representation; this gives κu_i.

The symmetric square of the standard representation decomposes as the direct sum of the trivial representation and one copy of the standard representation. The normalization $\sum_i w_i = 1$ removes the trivial component. Hence there is one quadratic equivariant degree of freedom, which may be represented by

$$u_i^2 - \frac{1}{3} \sum_j u_j^2.$$

This proves (28). ☐

5.1 The equilateral slope bound

Choose the standard equilateral triangle

$$A = (0, 0), \qquad B = (1, 0), \qquad C = \left(\frac{1}{2}, \frac{\sqrt{3}}{2} \right). \tag{29}$$

Using (28) and differentiating with respect to A gives

$$S_A = \begin{pmatrix} \frac{1}{3} - \frac{\kappa}{4} & -\frac{\sqrt{3}\kappa}{4} \\ -\frac{\sqrt{3}\kappa}{4} & \frac{1}{3} + \frac{\kappa}{4} \end{pmatrix}. \tag{30}$$

Its eigenvalues are

$$\frac{1}{3} + \frac{\kappa}{2}, \qquad \frac{1}{3} - \frac{\kappa}{2}. \tag{31}$$

Theorem 5.2 (Equilateral slope and boundary-curvature constraints)**.** *For every C^1 attractive invariant triangle center whose weights are analytic at the equilateral triangle,*

$$\boxed{|\kappa| \le \frac{2}{3}.} \tag{32}$$

If equality holds and the second-order coefficient in (28) exists, then

$$\boxed{\kappa = \frac{2}{3} \Longrightarrow \eta = 2, \qquad \kappa = -\frac{2}{3} \Longrightarrow \eta = -\frac{10}{3}.} \tag{33}$$

Proof. The eigenvalues (31) prove (32). For the endpoint constraints, perturb the third vertex by

$$C = \left(\frac{1}{2} + r, \frac{\sqrt{3}}{2} + t\right).$$

At $\kappa = 2/3$, the zero eigendirection of (30) is $v_+ = (\sqrt{3}/2, 1/2)$. The first variation of its Rayleigh quotient is

$$v_+^T\,\delta S_A\,v_+ = (\eta - 2)\left(\frac{r}{4} - \frac{\sqrt{3}\,t}{12}\right). \tag{34}$$

Both signs of (r, t) occur inside the nondegenerate shape domain, so local positive semidefiniteness is impossible unless $\eta = 2$.

At $\kappa = -2/3$, a unit null vector is $v_- = (-1/2, \sqrt{3}/2)$ and

$$v_-^T\,\delta S_A\,v_- = (3\eta + 10)\left(\frac{r}{12} - \frac{\sqrt{3}\,t}{36}\right). \tag{35}$$

The same two-sided argument gives $\eta = -10/3$. □

Geometric proof from the isosceles chest. There is a second proof which explains the numerical endpoint coefficients. Use the isosceles family

$$T_h = \{(0,h), (-1,0), (1,0)\}, \qquad h = \sqrt{3} + \delta.$$

For a center with expansion (28), direct substitution of $a = 2$ and $b = c = \sqrt{1+h^2}$ gives

$$y_X(h) = \frac{1}{\sqrt{3}} + \left(\frac{1}{3} - \frac{\kappa}{2}\right)\delta + \sqrt{3}\left(\frac{\eta}{24} - \frac{\kappa}{8}\right)\delta^2 + O(\delta^3). \tag{36}$$

By the exact isosceles chest theorem of Paper II [2], every ambiently attractive center is confined between the constant geometric-median branch $1/\sqrt{3}$ and

$$y_\infty(h) = \frac{h^2 - 1}{2h} = \frac{1}{\sqrt{3}} + \frac{2}{3}\delta - \frac{\sqrt{3}}{18}\delta^2 + O(\delta^3)$$

on both sides of $\delta = 0$, with the order of the endpoints reversed when δ changes sign. Comparing first-order coefficients gives $0 \le 1/3 - \kappa/2 \le 2/3$, hence $|\kappa| \le 2/3$. If $\kappa = 2/3$, the first-order term agrees with the constant endpoint and the quadratic term must vanish on both sides, giving $\eta = 2$. If $\kappa = -2/3$, the quadratic coefficient must equal that of y_∞, giving $\eta = -10/3$. □

The slope bound is a purely local necessary condition, but it is extremely cheap. Any proposed center whose prepared analytic weights violate it is non-attractive without requiring a scan of distant triangle shapes.

Corollary 5.3 (Kimberling center-function slope test)**.** *Suppose unnormalized barycentric weights are generated cyclically by a smooth center function $f(a,b,c)$ with $f(a,b,c) = f(a,c,b)$ and $f(1,1,1) = f_0 \neq 0$. Set*

$$\alpha = \left.\frac{\partial f}{\partial \log a}\right|_{(1,1,1)}, \qquad \beta = \left.\frac{\partial f}{\partial \log b}\right|_{(1,1,1)}.$$

Then

$$\kappa = \frac{\alpha - \beta}{3 f_0}. \tag{37}$$

Hence attractivity requires

$$|\alpha - \beta| \le 2|f_0|. \tag{38}$$

Proof. For a zero-sum logarithmic perturbation u, symmetry gives $\delta f_A = (\alpha - \beta)u_a$. The first variation of the cyclic denominator vanishes because $u_a + u_b + u_c = 0$. Normalization therefore gives (37). □

5.2 Benchmarks

For the centroid,

$$(\kappa, \eta) = (0, 0).$$

For the incenter, $w_i = e^{u_i} / \sum_j e^{u_j}$, so

$$(\kappa, \eta) = \left(\frac{1}{3}, \frac{1}{6}\right). \tag{39}$$

For $X(10)$,

$$w_i = \frac{1}{2} - \frac{1}{2}\frac{e^{u_i}}{\sum_j e^{u_j}},$$

and therefore

$$(\kappa, \eta) = \left(-\frac{1}{6}, -\frac{1}{12}\right). \tag{40}$$

These lie comfortably inside the necessary slope interval.

To first order in a small shape perturbation, every analytic attractive center therefore lies on the single affine direction

$$X - G = \kappa \sum_i u_i p_i + O(\|u\|^2), \qquad |\kappa| \le \frac{2}{3}. \tag{41}$$

For each fixed analytic rule, the leading displacement therefore lies in this one-dimensional direction and any transverse term starts at second order. This is a pointwise-in-rule statement. A uniform thickness or area asymptotic for the entire attainable locus would additionally require uniform Taylor remainder bounds over the chosen class, which are not proved here.

5.3 Third-order refinement from the isosceles chest

The representation theory remains one-dimensional at cubic order.

Proposition 5.4 (Universal cubic term)**.** *For an analytic invariant triangle center, the expansion* (28) *extends uniquely at cubic order to*

$$w_i = \frac{1}{3} + \kappa u_i + \eta\left(u_i^2 - \frac{1}{3}R_2\right) + \zeta R_2 u_i + O(\|u\|^4), \qquad R_2 = \sum_j u_j^2. \tag{42}$$

There is no second independent zero-sum S_3-equivariant cubic term.

Proof. The space of homogeneous cubic equivariant maps from the standard two-dimensional representation of S_3 to itself has multiplicity one. The nonzero covariant $u \mapsto R_2 u$ therefore spans it. Normalization removes the trivial component as at second order. □

For the isosceles deformation $h = \sqrt{3} + \delta$, (42) gives

$$\begin{aligned} y_X(h) = \frac{1}{\sqrt{3}} &+ \left(\frac{1}{3} - \frac{\kappa}{2}\right)\delta + \sqrt{3}\left(\frac{\eta}{24} - \frac{\kappa}{8}\right)\delta^2 \\ &+ \left(\frac{\eta}{48} + \frac{\kappa}{24} - \frac{\zeta}{16}\right)\delta^3 + O(\delta^4). \end{aligned} \tag{43}$$

Meanwhile

$$\frac{h^2 - 1}{2h} = \frac{1}{\sqrt{3}} + \frac{2}{3}\delta - \frac{\sqrt{3}}{18}\delta^2 + \frac{1}{18}\delta^3 + O(\delta^4). \tag{44}$$

Corollary 5.5 (Cubic endpoint constraints)**.** *At the two extremal second-order jets forced by Theorem 5.2, ambient attractivity implies*

$$\boxed{(\kappa, \eta) = \left(\frac{2}{3}, 2\right) \Longrightarrow \zeta \leq \frac{10}{9}, \qquad (\kappa, \eta) = \left(-\frac{2}{3}, -\frac{10}{3}\right) \Longrightarrow \zeta \geq -\frac{22}{9}.} \tag{45}$$

Equality corresponds formally to following the M_1 and M_∞ endpoint branches, respectively.

Proof. For $(\kappa, \eta) = (2/3, 2)$, the first two nonconstant coefficients in (43) vanish. The isosceles chest requires the cubic coefficient to be nonnegative on both sides in the appropriate oriented sense:

$$\frac{5}{72} - \frac{\zeta}{16} \geq 0,$$

which is $\zeta \leq 10/9$.

For $(\kappa, \eta) = (-2/3, -10/3)$, subtract (44) from (43). The first nonzero possible difference is

$$\left(-\frac{11}{72} - \frac{\zeta}{16}\right) \delta^3.$$

The endpoint order reverses with the sign of δ, so the coefficient must be nonpositive, giving $\zeta \geq -22/9$. □

The variational power family provides a useful geometric comparison with the formal endpoint jets, but its detailed higher-order coefficient formulas are not needed below. The global attractivity theory of this family, including the exact exponent interval and singular configurations, is developed in Paper III [3].

6 A complete polynomial covariant basis for analytic constructions

The normalized squared-side variables (4) make it possible to organize analytic families systematically instead of guessing unrelated center functions. The language is standard finite-group invariant theory; see, for example, Sturmfels [12].

Define the two zero-sum covariants

$$v_i^{(1)} = s_i - \frac{1}{3}, \tag{46}$$

$$v_i^{(2)} = s_i^2 - \frac{s_1^2 + s_2^2 + s_3^2}{3}. \tag{47}$$

Theorem 6.1 (Polynomial covariant module)**.** *Let $F = (F_1, F_2, F_3)$ be a polynomial map in (s_1, s_2, s_3) satisfying*

$$F(\sigma s) = \sigma F(s) \qquad (\sigma \in S_3), \qquad F_1 + F_2 + F_3 = 0.$$

Then there exist symmetric polynomials $A(e_1, e_2, e_3)$ and $B(e_1, e_2, e_3)$ such that

$$F_i = A\left(s_i - \frac{e_1}{3}\right) + B\left(s_i^2 - \frac{e_1^2 - 2e_2}{3}\right), \tag{48}$$

where $e_1 = s_1 + s_2 + s_3$. On the normalized shape plane $e_1 = 1$, the module of zero-sum polynomial covariants is therefore generated by $v^{(1)}$ and $v^{(2)}$ over the symmetric polynomial ring in e_2, e_3.

Proof. By equivariance, F_1 is invariant under interchange of s_2 and s_3. Hence it is a polynomial in

$$s_1, \qquad s_2 + s_3 = e_1 - s_1, \qquad s_2 s_3 = e_2 - s_1(e_1 - s_1).$$

Thus F_1 is a polynomial in s_1, e_1, e_2. Using the cubic identity

$$s_1^3 - e_1 s_1^2 + e_2 s_1 - e_3 = 0,$$

reduce it to

$$F_1 = A_0 + A_1 s_1 + A_2 s_1^2$$

with symmetric polynomial coefficients. Equivariance gives the same formula for every F_i. Summing over i and using $\sum_i F_i = 0$ gives

$$3A_0 + A_1 e_1 + A_2(e_1^2 - 2e_2) = 0,$$

which is exactly (48). $\square$

This theorem justifies the type of basis used in the original computational experiments: it is not merely a convenient ansatz for polynomial weights; it is the complete polynomial equivariant form.

A finite analytic family can therefore be written

$$w_i = \frac{1}{3} + A(e_2, e_3) v_i^{(1)} + B(e_2, e_3) v_i^{(2)}, \tag{49}$$

with, for example,

$$A(e_2, e_3) = \sum_{j+k \le d} \alpha_{jk} (3e_2)^j (27e_3)^k,$$
$$B(e_2, e_3) = \sum_{j+k \le d} \beta_{jk} (3e_2)^j (27e_3)^k.$$

The factors are normalized to equal 1 at the equilateral point.

For fixed basis degree, the center value and every symmetric Jacobian block are affine in the coefficient vector

$$c = (\alpha_{jk}, \beta_{jk}).$$

Consequently sampled PSD constraints are linear matrix inequalities in c, and support optimization at a target triangle is a convex conic problem.

Remark 6.2 (From numerical to rigorous inner certificates)**.** A finite shape grid produces only candidate centers. A rigorous heart point requires a global proof of

$$S_i(s; c) \succeq 0 \qquad \text{for every } s \in \mathscr{S}.$$

The semialgebraic description (6) is useful here. After clearing positive denominators and introducing a polynomial representation of the oriented area where needed, one may use exact subdivision, interval arithmetic, or sum-of-squares certificates. Strictly positive candidates on a compact subdomain bounded away from degeneracy are particularly amenable to certification.

7 The first-jet semidefinite outer relaxation

Inner construction requires a global center function. For an outer bound on the smooth heart, however, one may forget global integrability and retain only necessary local first-order data. The resulting optimization is a small semidefinite program in the standard sense of convex optimization [14].

Fix a generic scalene target triangle with side lengths (a, b, c). Treat

$$w_A, w_B$$

and the four derivatives

$$\partial_a w_A, \quad \partial_b w_A, \qquad \partial_a w_B, \quad \partial_b w_B$$

as free variables. Set

$$w_C = 1 - w_A - w_B.$$

Differentiated normalization gives

$$\partial_k w_C = -\partial_k w_A - \partial_k w_B \qquad (k = a, b, c),$$

while degree-zero homogeneity gives, for each weight,

$$a\partial_a w_i + b\partial_b w_i + c\partial_c w_i = 0. \tag{50}$$

Thus every missing first derivative is affine in six free jet variables. Equations (7)–(8) then make each S_A, S_B, S_C affine in the same jet.

Definition 7.1 (First-jet relaxation)**.** Let $\mathcal{J}_1(P)$ be the projection to

$$x = w_A A + w_B B + w_C C$$

of the set of first jets satisfying

(J1) $w_A + w_B + w_C = 1$ and $w_i \geq 0$;

(J2) differentiated normalization and the homogeneity relations (50);

(J3) the three semidefinite constraints $S_A, S_B, S_C \succeq 0$;

(J4) every already proved value constraint desired from Paper I, for example $x \in \mathcal{C}_{\mathrm{std}}(P)$.

At targets with nontrivial symmetry, include all stabilizer covariance equations for the value and jet; in particular, equilateral symmetry fixes the value to the centroid.

Proposition 7.2 (Jet outer theorem)**.** *For every nondegenerate triangle,*

$$\mathcal{V}^1(P) \subseteq \mathcal{J}_1(P). \tag{51}$$

Moreover $\mathcal{J}_1(P)$ is a convex semidefinite-representable set, and its support function is computable by a finite SDP.

Proof. Every global C^1 attractive center supplies its true value and first derivatives at P. These satisfy all four groups of constraints, so its value lies in the projection. All constraints are affine equalities, linear inequalities, or affine 2×2 LMIs in the jet variables; hence the feasible set is a spectrahedron and its projection is a spectrahedral shadow. □

The inclusion can be strict. A feasible first jet need not continue around shape space to a single permutation-equivariant center function. Higher mixed derivatives, compatibility under continuation, and behavior near symmetry strata are absent from $\mathcal{J}_1$. Thus this construction is an outer relaxation of the smooth heart, not a method for manufacturing heart points.

Theorem 7.3 (Local first-jet relaxation is redundant off the equilateral shape)**.** *At a scalene triangle, every prescribed point of the plane is the value of a local real-analytic similarity- and permutation-invariant germ with $S_A = S_B = S_C = I/3$. At a non-equilateral isosceles triangle, the same statement holds for every value on its reflection axis. Consequently a local jet relaxation imposing nonnegative barycentric values and an outer chest adds no further value restriction at these targets. At an equilateral triangle, invariance instead forces the centroid.*

Proof. Use the normalized complex chart $z_0 = x + iy$, $y > 0$, and prescribe $w \in \mathbb{C}$. Put

$$a = \frac{1}{3} + i\,\frac{(1+x)/3 - \Re w}{y}, \qquad f(z) = w + a(z - z_0).$$

For the induced directly similarity-equivariant map $X(A,B,C) = A+(B-A)f((C-A)/(B-A))$, the three complex-linear response coefficients are a, $f - za$, and $1 - f + (z-1)a$. Their real parts are all $1/3$ throughout this branch. The anti-holomorphic derivatives vanish, so all symmetric response blocks equal $I/3$. For a scalene target choose a neighbourhood in labelled shape space disjoint from its distinct relabellings and reflected relabellings, and define the other branches by covariance. This is a local invariant germ, not a globally defined center. For an isosceles target choose the base normalization $z_0 = 1/2 + iy$ and $w = 1/2 + iv$. Then $a = 1/3$ and $f(z) = z/3 + 1/3 + i(v - y/3)$ obeys $f(1-\bar{z}) = 1 - \overline{f(z)}$, the stabilizer compatibility condition. The other local branches are again defined by covariance. The equilateral stabilizer is larger and forces the centroid, so this construction does not apply there. Value nonnegativity now cuts the admissible prescribed values to the hull, and an inserted chest cuts them exactly to that chest. □

These are actual analytic germs, so their derivatives satisfy every finite order of local compatibility. Merely increasing the jet order at one target cannot remove these locally realizable values. Useful refinements must couple distinct shapes, for example by finite displacement inequalities, transport of the same function between charts, and boundary conditions. This does not make global semidefinite optimization of a shared polynomial family redundant: its coefficients couple all shapes and its positivity must still be proved globally.

8 Exploratory ETC evidence and reproducibility status

The Encyclopedia of Triangle Centers (ETC) is an unusually large source of explicit barycentric and trilinear formulas [4, 5]. It is therefore valuable for discovery, but no finite scan can establish global attractivity. We use the computation in this paper only as exploratory reconnaissance.

A corrected survivor-biased retest considered $2,428$ distinct ETC indices: $2,207$ centers surviving an earlier screen among $X(1), \ldots, X(11799)$ and 221 earlier execution failures. The final statuses were

status	number
survived both the corrected Jacobian test and the isosceles filter	594
numerical negative-eigenvalue witness found	1,762
additional isosceles/convex-hull violation	38
inadmissible on a sampled singular shape	1
unresolved	33

The population is deliberately survivor-biased, so 594/2428 has no frequency interpretation. The isosceles test is not merely a fitted extrapolation: at $h = 10^{-6}$ the same 38 formulas already have direct 50-digit values outside $[0, 1]$, ranging approximately from -5.77×10^5 to 3.85×10^5. Paper II proves the underlying finite-height and asymptotic chest inequalities [2].

For reproducibility, the 38 newly excluded ETC indices are

2047, 5459, 6304, 6306, 6669, 6671, 6673, 6694, 6695, 7375, 7376, 7388, 7389, 8180, 8320, 11289, 11290, 11291, 11292, 11294, 11295, 11297, 11298, 11299, 11301, 11303, 11304, 11305, 11306, 11307, 11308, 11309, 11311, 11312, 11313, 11314, 11315, 11316.

The supplement contains the historical tested-index and endpoint tables, the numerical search code, repaired scan drivers, and an independent table audit with assertions. It also bundles the locally available ETC database and expression expander with their hashes and repository metadata, under the repository's included license. The historical run did not record its source snapshot, so the bundle does not assert identity with the historical generating database. Fresh witness checks must cite the supplied snapshot explicitly. Stored high-precision negative values remain numerical witnesses until their sign is verified exactly or enclosed rigorously. None of the counts proves global attractivity or a limiting value. The supplement's replay driver saves full-precision expressions and witnesses for subsequent certification.

9 A genuinely two-dimensional analytic heart

The certified segment (27) does not by itself show that a triangle heart has area. We now add a second, independent attractive family.

For $p > 1$, let

$$M_p(P) = \arg\min_{x\in\mathbb{R}^2} \sum_{i=1}^{3} \|x - p_i\|^p.$$

Paper III proves, with a complete treatment of singular configurations, that M_p is globally attractive exactly for

$$4 - 2\sqrt{2} \le p \le 4 + 2\sqrt{2}$$

within the power family, and more generally classifies smooth strictly convex radial location functionals by their force elasticity [3]. Only the existence of an open globally attractive interval through $p = 2$ is needed here.

9.1 The tangent of the power-center curve at the centroid

Let

$$r_i = |G - p_i|.$$

Differentiating the equilibrium equation at $p = 2$ gives the following formula; the same Hessian-inverse implicit-differentiation structure occurs in general Fréchet-mean differentiation [11]:

$$\boxed{V(P) := \left.\frac{\partial M_p(P)}{\partial p}\right|_{p=2} = \frac{1}{3}\sum_{i=1}^{3} \log r_i\,(p_i - G).} \tag{52}$$

The common additive constant in the three logarithms is irrelevant because $\sum_i (p_i - G) = 0$.

Put

$$L(P) = X(10)(P) - G(P), \qquad D(P) = \det(L(P), V(P)).$$

Both are real-analytic functions on the nondegenerate labelled triangle domain.

Theorem 9.1 (Generic nonempty interior of the analytic heart)**.** *The function D is not identically zero. Consequently the set of triangle shapes for which*

$$D(P) \neq 0$$

is open and dense. For every such triangle, the analytic attainable locus $\mathcal{V}^{\omega}(P)$ has nonempty interior.

Proof. We first show that D is not identically zero by one exact shape. Choose centroid-zero vertices

$$p_1 = (1, 0), \qquad p_2 = \left(\frac{29}{32}, \frac{\sqrt{1463}}{32}\right), \qquad p_3 = \left(-\frac{61}{32}, -\frac{\sqrt{1463}}{32}\right). \tag{53}$$

Their distances from the centroid are

$$1, \qquad \frac{3}{2}, \qquad \frac{9}{4},$$

so (52) becomes

$$V = \frac{\log(3/2)}{3}(p_2 + 2p_3) = \frac{\log(3/2)}{96}(-93, -\sqrt{1463}). \tag{54}$$

The side lengths are

$$\frac{\sqrt{218}}{4}, \qquad \frac{\sqrt{158}}{4}, \qquad \frac{\sqrt{23}}{4}.$$

A direct substitution into (19) gives

$$\det\big(X(10), p_2 + 2p_3\big) = -\frac{-\sqrt{318934} - \sqrt{33649} + 2\sqrt{231154}}{64(\sqrt{23} + \sqrt{158} + \sqrt{218})}, \tag{55}$$

which is nonzero. Indeed equality of the numerator to zero would imply, after one squaring,

$$572033^2 = 4 \cdot 318934 \cdot 33649,$$

whereas the two sides differ by 284294512425. Since $\log(3/2) > 0$, (54) proves $D(P) \neq 0$ for this triangle.

Thus the real-analytic function D is not identically zero; the standard zero-set theorem for real-analytic functions implies that its zero set has empty interior, and the nonzero set is open and dense [13].

Now fix P with $D(P) \neq 0$. By analyticity in p,

$$M_p(P) = G + (p-2)V(P) + O((p-2)^2).$$

For all sufficiently small nonzero $p - 2$, $M_p(P)$ is therefore not on the affine line through $X(1), G, X(10)$. Choose such a p inside the globally attractive exponent interval of Paper III. The three analytic attractive centers $X(1)$, $X(10)$, and M_p have noncollinear values at P. Convex mixing of the three center maps fills their ordinary triangle, a two-dimensional subset of $\mathcal{V}^{\omega}(P)$. Hence the analytic heart has nonempty interior. □

This result does not claim that every scalene triangle has a heart of positive area; it proves the property on an open dense set and identifies a concrete mechanism generating area.

9.2 The 13–20–21 diagnostic triangle

For continuity with Paper I, take

$$A = (0, 0), \qquad B = (21, 0), \qquad C = (5, 12).$$

Then

$$\begin{aligned} G &= (8.66666667, 4), \\ X(1) &= (7, 4.66666667), \\ X(10) &= (9.5, 3.66666667), \\ M_3 &\approx (9.48485511, 3.60076608). \end{aligned}$$

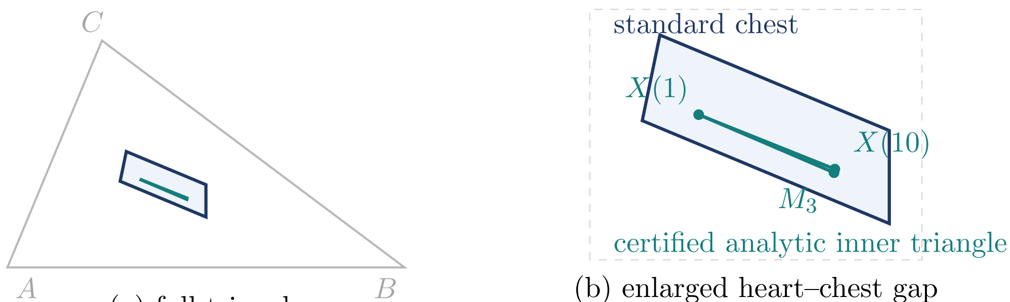

Figure 1: Actual inner–outer geometry for the diagnostic triangle $A = (0, 0)$, $B = (21, 0)$, $C = (5, 12)$ (side lengths $13, 20, 21$). The blue quadrilateral is Paper I's standard chest. The green triangle is the certified analytic inner set $\mathrm{conv}\{X(1), X(10), M_3\}$. Panel (b) enlarges the small region where the present inner and outer bounds differ.

The certified heart triangle

$$\mathrm{conv}\{X(1), X(10), M_3\}$$

has area approximately

$$0.08994818,$$

which is 0.07139% of the area 126 of the original triangle. Paper I's standard chest has area 7.47204, or 5.9302% of the original triangle. The large gap between these two certified numbers is not a contradiction: it measures how far the present inner constructions remain from the best known outer confinement.

10 Inner–outer support matching

The previous sections now give three mathematically distinct computational objects for a fixed target triangle P:

(1) a *proved outer chest*, such as $\mathcal{C}_{\mathrm{std}}(P)$ from Paper I;

(2) a *smooth first-jet outer relaxation* $\mathcal{J}_1(P)$;

(3) an *inner family* generated by globally certified analytic center maps, such as convex combinations of $X(1)$, $X(10)$, attractive M_p, and certified polynomial-covariant families.

For a unit direction n, define

$$\begin{aligned} h_{\mathrm{in}}(n) &= \sup\{n \cdot X(P) : X \text{ in the certified inner family}\}, \\ h_{\mathrm{jet}}(n) &= \sup\{n \cdot x : x \in \mathcal{J}_1(P)\}, \\ h_{\mathrm{chest}}(n) &= \sup\{n \cdot x : x \in \mathcal{C}_{\mathrm{std}}(P)\}. \end{aligned}$$

Then rigorously

$$h_{\mathrm{in}}(n) \le h_P^{\omega}(n) \le h_P^{1}(n) \le \min\{h_{\mathrm{jet}}(n), h_{\mathrm{chest}}(n)\}. \tag{56}$$

Whenever the left and right sides coincide, an exact supporting value of the closed analytic attainable locus is identified. An attained inner value gives a contact point; it is exposed only when the supporting face is a singleton.

Figure 1 replaces a schematic inclusion picture by the actual best currently quoted inner and outer sets for the diagnostic triangle. It suggests a practical hierarchy. Increase the polynomial-covariant basis degree from inside, while strengthening finite displacement networks coupling distinct shapes from outside. Local jets at one target alone cannot close the gap. Directions in which the gap is largest indicate where a new analytic family or a new necessary inequality would have the greatest value.

11 Open problems

1. Determine the exact closed analytic heart of a generic triangle. Even a single non-equilateral shape for which all support directions are matched would be a substantial result.
2. Decide whether
$$\overline{\mathcal{V}^{\omega}(P)} = \overline{\mathcal{V}^{\infty}(P)} = \overline{\mathcal{V}^{1}(P)}$$
for every nondegenerate triangle.
3. Determine whether the local slope bounds $-2/3 \leq \kappa \leq 2/3$ are sharp in the global analytic class. In particular, do globally attractive analytic centers exist with κ arbitrarily close to either endpoint?
4. Continue the Taylor analysis beyond the cubic constraints obtained here. At the two extremal jets, determine the fourth- and higher-order compatibility conditions forced by positivity on both sides of the equilateral shape.
5. Prove global PSD certificates for optimized polynomial-covariant families (49). Determine whether increasing degree is dense, in an appropriate topology, in the strictly attractive analytic class on compact subdomains of shape space.
6. Develop nonlocal outer systems coupling values and derivatives at multiple shapes through finite displacement constraints. Theorem 7.3 rules out recovering the heart by purely local jets at one target.
7. Extend the supplied reproducibility archive by certifying saved ETC witness signs and executing a fresh versioned survey with the equilateral and isosceles filters. The historical snapshot identity remains unverified.
8. Determine whether the $X(1)$–$X(10)$ segment is exposed on any portion of the true heart boundary for specified triangle shapes, or whether other attractive centers always extend beyond it in the same support directions.
9. Quantify the generic heart area and compare it with Paper I's standard chest area. Near the equilateral shape, derive the first nonzero asymptotic coefficient of the heart area.
10. Extend the smooth-heart machinery to four points, where barycentric weights are no longer functions of only three side lengths and the shape space has substantially higher dimension.

12 Conclusion

The centroid provides a natural affine origin for the global geometry of smooth triangle centers. Along every smooth center direction, attractivity reduces to an exact spectral interval. On the line generated by the boundary-wire center this interval is completely solvable and gives the sharp globally attractive family from the incenter through the centroid to $X(10)$.

Near the equilateral triangle, permutation symmetry forces universal second- and third-order barycentric jets and imposes necessary semidefinite constraints on their coefficients. Globally, normalized squared-side variables turn polynomial equivariant perturbations into a two-generator module over symmetric invariants. This supplies a systematic construction language and globally coupled semidefinite construction problems rather than a catalogue of isolated triangle-center formulas.

The analytic Heart is genuinely two-dimensional: Paper III supplies an open interval of globally attractive power centers through the centroid, and its tangent direction is generically transverse to the $X(1)$–$X(10)$ line. The unresolved problem is therefore the exact boundary.

Progress requires a controlled squeeze between globally certified analytic families from inside and nonlocal chest support bounds from outside. The corrected ETC survey illustrates how symbolic necessary conditions can cheaply remove false numerical survivors, but no finite catalogue can replace this global analytic problem.

A Derivation of the equilateral second-order constraints

For completeness we record the matrices behind Theorem 5.2. At the equilateral triangle (29), the gradients with respect to A of the centered logarithmic side variables are

$$\nabla_A u_a = \left(\frac{1}{2}, \frac{\sqrt{3}}{6}\right),$$
$$\nabla_A u_b = \left(0, -\frac{\sqrt{3}}{3}\right),$$
$$\nabla_A u_c = \left(-\frac{1}{2}, \frac{\sqrt{3}}{6}\right).$$

Substitution into (7) yields (30).

Now write

$$C = \left(\frac{1}{2} + r, \frac{\sqrt{3}}{2} + t\right).$$

The first derivatives of S_A with respect to r and t at the equilateral shape are

$$\frac{\partial S_A}{\partial r} = \begin{pmatrix} \frac{\eta}{4} - \frac{5\kappa}{4} & \frac{\sqrt{3}\kappa}{4} \\ \frac{\sqrt{3}\kappa}{4} & \frac{\eta}{4} - \frac{3\kappa}{4} \end{pmatrix} \tag{57}$$

and

$$\frac{\partial S_A}{\partial t} = \begin{pmatrix} \frac{\sqrt{3}(-\eta+5\kappa)}{12} & -\frac{\kappa}{4} \\ -\frac{\kappa}{4} & \frac{\sqrt{3}(-\eta+3\kappa)}{12} \end{pmatrix}. \tag{58}$$

At $\kappa = 2/3$, evaluation on $v_+ = (\sqrt{3}/2, 1/2)$ gives

$$v_+^T \frac{\partial S_A}{\partial r} v_+ = \frac{\eta - 2}{4}, \qquad v_+^T \frac{\partial S_A}{\partial t} v_+ = -\frac{\sqrt{3}(\eta - 2)}{12}.$$

At $\kappa = -2/3$, evaluation on $v_- = (-1/2, \sqrt{3}/2)$ gives

$$v_-^T \frac{\partial S_A}{\partial r} v_- = \frac{3\eta + 10}{12}, \qquad v_-^T \frac{\partial S_A}{\partial t} v_- = -\frac{\sqrt{3}(3\eta + 10)}{36}.$$

This proves (34)–(35).

References

[1] I. Hammoudeh, *Attractive Centers I: Chests, Hearts, and Symmetry–Displacement Geometry*, companion manuscript, 2026.

[2] I. Hammoudeh, *Attractive Centers II: Isosceles Geometry, Local Admissibility, and Global Extension*, companion manuscript, 2026.

[3] I. Hammoudeh, *Attractive Centers III: Radial Location Functionals, Mechanical Response, and an Exact Elasticity Classification*, companion manuscript, 2026.

[4] C. Kimberling, *Triangle Centers and Central Triangles*, Congressus Numerantium 129, Utilitas Mathematica Publishing, 1998.

[5] C. Kimberling, *Encyclopedia of Triangle Centers*, University of Evansville, `https://faculty.evansville.edu/ck6/encyclopedia/`, accessed September 2026.

[6] R. Pérez-Fernández, B. De Baets, and M. Gagolewski, A taxonomy of monotonicity properties for the aggregation of multidimensional data, *Information Fusion* **52** (2019), 322–334.

[7] M. Fréchet, Les èléments aléatoires de nature quelconque dans un espace distancié, *Annales de l'Institut Henri Poincaré* **10** (1948), 215–310.

[8] E. Weiszfeld, Sur le point pour lequel la somme des distances de n points donnés est minimum, *Tohoku Mathematical Journal* **43** (1937), 355–386.

[9] E. Welzl, Smallest enclosing disks (balls and ellipsoids), in H. Maurer (ed.), *New Results and New Trends in Computer Science*, Lecture Notes in Computer Science 555, Springer, 1991, 359–370.

[10] G. C. Shephard, The Steiner point of a convex polytope, *Canadian Journal of Mathematics* **18** (1966), 1294–1300.

[11] A. Lou, I. Katsman, Q. Jiang, S. Belongie, S.-N. Lim, and C. De Sa, Differentiating through the Fréchet mean, *Proceedings of the 37th International Conference on Machine Learning*, PMLR **119** (2020), 6393–6403.

[12] B. Sturmfels, *Algorithms in Invariant Theory*, 2nd ed., Springer, Vienna, 2008.

[13] S. G. Krantz and H. R. Parks, *A Primer of Real Analytic Functions*, 2nd ed., Birkhäuser, Boston, 2002.

[14] S. Boyd and L. Vandenberghe, *Convex Optimization*, Cambridge University Press, Cambridge, 2004.